

OCEAN g -MODES ON TRANSIENT NEUTRON STARS

ALEX DEIBEL^{1,2}

¹Department of Physics and Astronomy, Michigan State University, East Lansing, MI 48824, USA; deibel@msu.edu

²The Joint Institute for Nuclear Astrophysics - Center for the Evolution of the Elements, Michigan State University, East Lansing, MI 48824, USA

Draft version June 21, 2021

ABSTRACT

The neutron star ocean is a plasma of ions and electrons that extends from the base of the neutron star’s envelope to a depth where the plasma crystallizes into a solid crust. During an accretion outburst in an X-ray transient, material accumulates in the envelope of the neutron star primary. This accumulation compresses the neutron star’s outer layers and induces nuclear reactions in the ocean and crust. Accretion-driven heating raises the ocean’s temperature and increases the frequencies of g -modes in the ocean; when accretion halts, the ocean cools and ocean g -mode frequencies decrease. If the observed low-frequency quasi-periodic oscillations on accreting neutron stars are g -modes in the ocean, the observed quasi-periodic oscillation frequencies will increase during outburst—reaching a maximum when the ocean temperature reaches steady state — and subsequently decrease during quiescence. For time-averaged accretion rates during outbursts between $\langle \dot{M} \rangle = 0.1\text{--}1.0 \dot{M}_{\text{Edd}}$ the predicted g -mode fundamental $n = 1$ $l = 2$ frequency is between $\approx 3\text{--}7$ Hz for slowly rotating neutron stars. Accreting neutron stars that require extra shallow heating, such as the Z-sources MAXI J0556-332, MXB 1659-29, and XTE J1701-462, have predicted g -mode fundamental frequencies between $\approx 3\text{--}16$ Hz. Therefore, observations of low-frequency quasi-periodic oscillations between $\approx 8\text{--}16$ Hz in these sources, or in other transients that require shallow heating, will support a g -mode origin for the observed quasi-periodic oscillations.

Subject headings: dense matter – stars: neutron – X-rays: individual (MAXI J0556-332, MXB 1659-29, XTE J1701-462)

1. INTRODUCTION

The Z-sources are the most luminous neutron star X-ray transients ($L_X \sim 0.5\text{--}1.0 L_{X,\text{Edd}}$), with inferred mass accretion rates on the order of the Eddington accretion rate, as determined from the X-ray flux. These sources trace out a Z-shaped track in the X-ray color-color diagram (Hasinger & van der Klis 1989); the track is composed of the horizontal (top), normal (diagonal), and flaring (bottom) branches. During an accretion outburst, a source may vary its spectral state (its location on the “Z”) over the course of hours or days due to accretion instabilities at a nearly constant accretion rate (Lin et al. 2009; Homan et al. 2010; Fridriksson et al. 2015). Although changes in spectral state were thought to result from variations in the mass accretion rate, it is likely that accretion rate variations cause secular evolution of the source; for example, XTE J1701-462 transitioned into a lower luminosity atoll phase ($L_X \sim 0.1\text{--}0.5 L_{X,\text{Edd}}$) when its accretion rate decreased (Lin et al. 2009; Homan et al. 2010).

On the normal branch, low-frequency quasi-periodic oscillations between $\approx 5\text{--}7$ Hz are observed in several Z-sources, for example, Cyg X-2 (Hasinger & van der Klis 1989; Wijnants et al. 1997; Dubus et al. 2004), SCO X-1 (Hertz et al. 1992; van der Klis et al. 1996; Titarchuk et al. 2014), and GX 5-1 (Kuulkers et al. 1994; Jonker et al. 2002). The normal branch oscillation frequencies (hereafter NBOs) are consistent with g -modes (Bildsten & Cutler 1995; Bildsten et al. 1996) in the neutron star’s ocean — a plasma of ions and electrons that extends from the overlying envelope to the deeper crust — provided that the neutron star is slowly rotating ($\nu_{\text{spin}} \lesssim 10$ Hz). Low-frequency quasi-periodic oscillations are also consistent with being of a geometric origin (Stella & Vietri 1998; Homan 2012; Homan et al. 2015) from Lense–Thirring precession of an inner accretion disk

(Lense & Thirring 1918; Bardeen & Petterson 1975); for example, horizontal branch oscillation frequencies are consistent with a warped accretion disk geometry (Jonker et al. 2002). It has been difficult, however, to delineate the origin of the low-frequency NBOs given the uncertainties that remain in the nature of the accretion flow near the neutron star surface.

The thermal evolution of the neutron star ocean offers an opportunity to test for the presence of ocean g -modes by comparing the temporal evolution of predicted g -modes and observed NBOs. During an accretion outburst, the accumulation and compression of matter in the neutron star’s envelope induces nuclear reactions in the ocean and crust (Bisnovatyi-Kogan & Chechetkin 1979; Sato 1979) that deposit $\approx 1\text{--}2$ MeV per accreted nucleon (Haensel & Zdunik 1990). As the ocean’s temperature increases away from thermal equilibrium with the core, the predicted ocean g -mode frequencies also increase. When accretion ceases, the ocean cools back toward thermal equilibrium with the core and predicted ocean g -mode frequencies decrease. For example, in sources with time-averaged accretion rates between $\langle \dot{M} \rangle = 0.5\text{--}1.0 \dot{M}_{\text{Edd}}$, the predicted fundamental g -mode frequency shifts from an initial value of ≈ 3 Hz in a cold ocean to $\approx 5\text{--}7$ Hz when the ocean reaches steady state near ≈ 160 days after accretion begins — NBO frequencies in the $\approx 5\text{--}7$ Hz range are observed within the same time frame, for example, in XTE J1701-462 (Homan et al. 2007, 2010).

Models of neutron star thermal relaxation naturally reproduce quiescent light curves of neutron star transients (e.g., Brown & Cumming 2009). As determined from their quiescent light curves, some neutron star transients require extra “shallow” heating during outburst from an unknown source to explain their high temperatures at the outset of quiescence (Brown & Cumming 2009; Deibel et al. 2015; Turlione et

al. 2015). A finite amount of shallow heating, for instance, the ≈ 1 MeV per accreted nucleon needed in MXB 1659-29, raises the ocean’s steady-state temperature and predicted g -mode frequencies may be $\gtrsim 7$ Hz in this source. For this reason, any observed NBO frequencies $\gtrsim 7$ Hz in Z-sources that require extra shallow heating, such as MAXI J0556-332 (Deibel et al. 2015), MXB 1659-29 (Brown & Cumming 2009), and XTE J1701-462 (Turlione et al. 2015), would provide an observational test for the presence of ocean g -modes. These sources have the largest predicted g -mode frequencies during outburst, reaching frequencies between ≈ 8 –16 Hz. Furthermore, because the neutron star’s quiescent luminosity is much smaller than the heating rate during outburst in these sources, the large ocean temperatures and g -mode frequencies remain for thousands of days into quiescence.

In this study, we examine the thermal evolution of Z-sources and the temporal evolution of the ocean’s predicted fundamental g -mode in MAXI J0556-332, MXB 1659-29, XTE J1701-462, and accreting neutron stars with accretion rates similar to the transient Z-sources. In Section 2, we outline our neutron star thermal evolution model and demonstrate the evolution of the ocean during an accretion outburst. In Section 3, we explore changes in the g -mode spectrum over the course of the modeled outbursts. We discuss our results in Section 4.

2. THE THERMAL EVOLUTION OF THE OCEAN

We follow the thermal evolution of the neutron star’s outer layers by solving the fully general relativistic heat diffusion equation using the open source code dStar (Brown 2015). The microphysics follow Brown & Cumming (2009) with changes outlined in Deibel et al. (2015). dStar uses the numerics package available as part of the open source stellar evolution code MESA (Paxton et al. 2011, 2013, 2015). Thermal evolution models have successfully modeled quiescent light curves for neutron star transients; for instance, EXO 0748-676 (Degenaar et al. 2009, 2014) and Swift J174805.3-244637 (Degenaar et al. 2015).

Some sources require additional heating during outburst to reconcile models with quiescent observations, for example, KS 1731-260 (Wijnands et al. 2001, 2002; Cackett et al. 2010) and MXB 1659-29 (Wijnands et al. 2003, 2004; Cackett et al. 2008) require $Q_{\text{shallow}} \approx 1$ MeV per accreted nucleon of extra heating in the shallow crust (Brown & Cumming 2009). A recent fit to the quiescent light curve of XTE J1701-462 (Fridriksson et al. 2010, 2011) requires a $Q_{\text{shallow}} \approx 0.2$ MeV per accreted nucleon heat source in its shallow crust (Turlione et al. 2015). The hottest neutron star transient, MAXI J0556-332 (Homan et al. 2011, 2014; Matsumura et al. 2011; Sugizaki et al. 2013), requires a $Q_{\text{shallow}} \approx 4$ –16 MeV per accreted nucleon heat source in its shallow crust to fit quiescent observations (Deibel et al. 2015).

Before the onset of accretion, the neutron star ocean is in thermal equilibrium with the core near $T_{\text{core}} \sim 10^7$ K, as inferred from cooling neutron star transients (Brown et al. 1998; Brown & Cumming 2009; Page & Reddy 2013). During active accretion, compression-induced nuclear reactions deposit ≈ 1 –2 MeV per accreted nucleon in the ocean and crust (Haensel & Zdunik 1990, 2003; Gupta et al. 2007; Haensel & Zdunik 2008) and the initially cold ocean can reach temperatures of $T_b \gtrsim 10^8$ K. Moreover, in sources that require shallow heating, the ocean temperature can reach $T_b \gtrsim 10^9$ K in steady state (Deibel et al. 2015). An increase

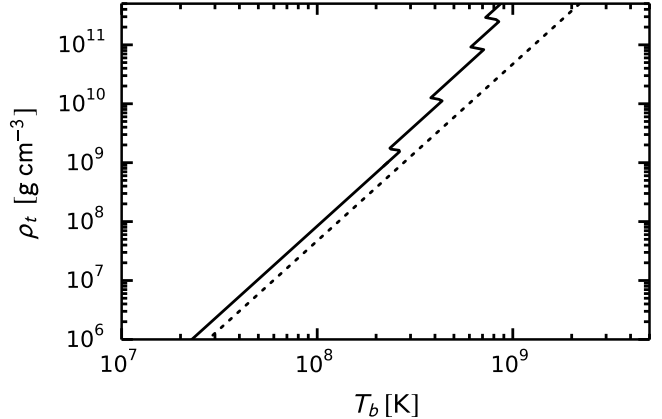


FIG. 1.— Location of the ocean-crust transition as a function of temperature at the base of the ocean. The black solid curve is for the one-component accreted composition (Haensel & Zdunik 1990) and the black dotted curve is for a multi-component accreted composition (Steiner 2012). The crystallization density is given by Equation (2).

in the temperature at the base of the ocean increases the crystallization depth of the ocean. The crystallization of the one-component ocean, with proton number Z , baryon number A , and ion number density n_i , depends on the plasma coupling parameter

$$\Gamma = \frac{(Ze)^2}{ak_B T_b}, \quad (1)$$

where T_b is the temperature at the base of the ocean, $a = (3/4\pi n_i)^{1/3}$ is the inter-ionic spacing, and the crystallization point occurs where $\Gamma = 175$ (Farouki & Hamaguchi 1993; Potekhin & Chabrier 2000). Therefore, the ocean-crust transition occurs at a mass density of

$$\rho_t \approx 2.2 \times 10^6 \text{ g cm}^{-3} \left(\frac{T_b}{3 \times 10^7 \text{ K}} \right)^3 \left(\frac{26}{Z} \right)^6 \left(\frac{A}{56} \right). \quad (2)$$

The ocean-crust transition density as a function of temperature can be seen in Figure 1. For simplicity, we use a one-component accreted composition (Haensel & Zdunik 1990) that roughly traces models of the multi-component accreted composition (Steiner 2012), as can be seen in Figure 1. Note that as the crust liquifies, composition changes in the solid crust become part of the liquid ocean. Sharp composition changes in the ocean, such as those arising from e^- -capture layers, can trap modes in the ocean (Bildsten & Cumming 1998) and decrease mode frequencies (Strohmayer 1993). We assume, however, that composition changes do not affect ocean oscillations because a realistic accreted composition contains smooth gradients in $\langle Z \rangle$ and $\langle A \rangle$ (Steiner 2012).

The timescale for changes to the ocean-crust transition density is related to the thermal time at the base of the ocean. We use the thermal time from Deibel et al. (2015; their Equation (1)),

$$\tau_{\text{therm, ocean}}^{\infty} \approx 1.0 \text{ days } \rho_9 \left(\frac{g_{14}}{2} \right)^{-2} \left(\frac{Y_e}{0.4} \right)^3 \left(\frac{Z}{26} \right) \left(\frac{1+z}{1.31} \right), \quad (3)$$

where Y_e is the electron fraction, $g_{14} \equiv g/10^{14} \text{ cm s}^{-2}$ is the gravitational acceleration with $g = (1+z)GM/R^2$, $1+z = (1-2GM/(Rc^2))^{-1/2}$ redshifts to an observer frame at infinity, and $\rho_9 \equiv \rho/(10^9 \text{ g cm}^{-3})$. The thermal time in the ocean as a function of mass density can be seen in Figure 2. The timescale for changes to the ocean-crust transition density is $\tau_t^{\infty} = (d \ln T / d \ln \rho_t) (dt / d \ln T) = \tau_{\text{therm, ocean}}^{\infty} / 3$.

MAXI J0556-332 is the hottest quiescent Z -source to date, and to reproduce the observed MAXI J0556-332 outburst beginning in 2011 (Matsumura et al. 2011) we run a model that accretes at $\langle \dot{M} \rangle = 1.0 \dot{M}_{\text{Edd}}$ for 16 months. We use the model parameters from the best fit to the quiescent light curve from Deibel et al. (2015): a neutron star mass $M = 1.5 M_{\odot}$, a neutron star radius $R = 11$ km, a core temperature $T_{\text{core}} = 3 \times 10^7$ K, an impurity parameter $Q_{\text{imp}} = 1$, and a shallow heat source of $Q_{\text{shallow}} = 6$ MeV per accreted nucleon. We assume the shallow heating varies proportionally with the accretion rate and is deposited over the column depth range $y = 2 \times 10^{13} - 2 \times 10^{14}$ g cm $^{-2}$ as inferred by the quiescent light curve (Deibel et al. 2015), where $y = P/g$ is the column depth.

In the model of the MAXI J0556-332 accretion outburst, the ocean temperature reaches $T_b \approx 7.5 \times 10^8$ K in steady state and the ocean-crust boundary moves from $\rho_t \approx 2.2 \times 10^6$ g cm $^{-3}$ to $\rho_t \approx 1.7 \times 10^{11}$ g cm $^{-3}$, as can be seen in Figure 3. Note that the ocean temperature increases relatively quickly during the outburst due to the combined heating from accretion-driven nuclear reactions and shallow heating, which deposit $L_{\text{nuc}} \approx 1.5 \times 10^{37}$ ergs s $^{-1}$. The quiescent luminosity of the neutron star, however, is only $L_q \approx 2.3 \times 10^{35}$ ergs s $^{-1}$, and the neutron star therefore cools over a period much longer than the outburst duration. As a consequence, the ocean remains $\geq 7 \times 10^8$ K for ≈ 500 days into quiescence and takes ≈ 2900 days to cool completely.

Motivated by renewed activity in MXB 1659-29 (Negoro et al. 2015), we explore its thermal evolution in a model representative of its previous 2.5 year outburst (Wijnands et al. 2003, 2004) near $\langle \dot{M} \rangle = 0.1 \dot{M}_{\text{Edd}}$. The model uses a neutron star mass of $M = 1.6 M_{\odot}$, a neutron star radius of $R = 11.2$ km, a core temperature of $T_{\text{core}} = 3 \times 10^7$ K, an impurity parameter of $Q_{\text{imp}} = 4$, and a $Q_{\text{shallow}} = 1$ MeV per accreted nucleon shallow heat source, which agrees with the quiescent light curve fit from Brown & Cumming (2009). During the accretion outburst, the ocean temperature reaches $T_b \approx 3.0 \times 10^8$ K and the ocean-crust boundary moves to $\rho_t \approx 3.6 \times 10^9$ g cm $^{-3}$. The outburst heating rate is $L_{\text{nuc}} \approx 2.7 \times 10^{35}$ ergs s $^{-1}$ and the quiescent luminosity of the neutron star is $L_q \approx 8.9 \times 10^{33}$ ergs s $^{-1}$. As a consequence, the ocean remains $T_b \geq 1.0 \times 10^8$ K for ≈ 700 days into quiescence and takes ≈ 1400 days to cool completely.

We also run a model of the XTE J1701-462 outburst (Fridriksson et al. 2010, 2011). The model uses a neutron star mass of $M = 1.6 M_{\odot}$, a neutron star radius of $R = 11.6$ km, a core temperature of $T_{\text{core}} = 3 \times 10^7$ K, an impurity parameter of $Q_{\text{imp}} = 7$, and a $Q_{\text{shallow}} = 0.17$ MeV per accreted nucleon shallow heat source, which agrees with the quiescent light curve fit from Turlione et al. (2015). During the accretion outburst, the ocean temperature reaches $T_b \approx 3.1 \times 10^8$ K and the ocean-crust boundary moves to $\rho_t \approx 3.9 \times 10^9$ g cm $^{-3}$. The outburst heating rate is $L_{\text{nuc}} \approx 2.1 \times 10^{36}$ ergs s $^{-1}$ and the quiescent luminosity of the neutron star is $L_q \approx 1.9 \times 10^{34}$ ergs s $^{-1}$. As a consequence, the ocean remains $T_b \geq 1.0 \times 10^8$ K for ≈ 1700 days into quiescence and takes ≈ 3100 days to cool completely.

We also run a series of models with various time-averaged accretion rates to investigate the possible g -mode spectrum in other Z -sources. We run models with time-averaged accretion rates during a Z -track cycle $\langle \dot{M} \rangle / \dot{M}_{\text{Edd}} = 0.1, 0.25, 0.5, 0.75$, and 1.0, for a 1 year outburst to approximate a typical Z -source outburst. We use a fiducial neutron star mass $M =$

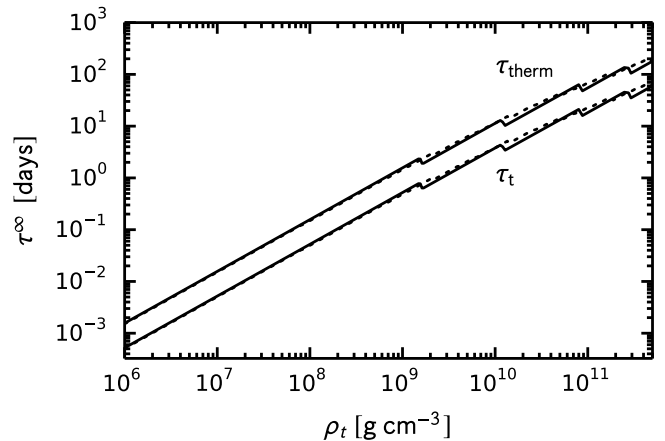


FIG. 2.— Characteristic timescales in the neutron star ocean. The upper curves are the thermal time for an equilibrium composition (solid curve) and accreted composition (dotted curve). The lower curves are for the timescale for changes in ρ_t for an equilibrium composition (solid curve) and an accreted composition (dotted curve).

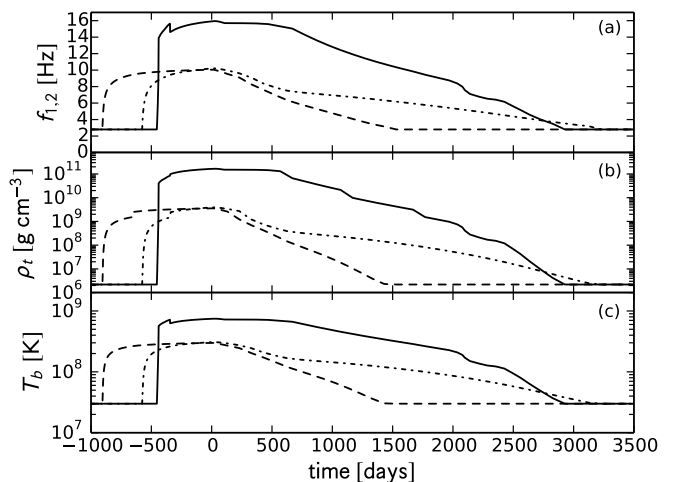


FIG. 3.— Thermal evolution as a function of time during outburst/quiescence for MAXI J0556-332 (solid curves), MXB 1659-29 (dashed curves), and XTE J1701-462 (dotted-dashed curves). Panel (a): fundamental $n = 1, l = 2$ g -mode frequencies in the ocean (Equation 4). Panel (b): the ocean-crust transition density (Equation 2). Panel (c): temperature at the ocean-crust transition.

$1.4 M_{\odot}$ and radius $R = 10$ km, with a core temperature $T_{\text{core}} = 3 \times 10^7$ K for all models. Models with time-averaged accretion rates between $\langle \dot{M} \rangle = 0.1 - 0.5 \dot{M}_{\text{Edd}}$ have ocean temperatures between $T_b \approx 4.5 \times 10^7 - 9.9 \times 10^7$ K and ocean-crust transition densities between $\rho_t \approx 7.5 \times 10^6 - 8.1 \times 10^7$ g cm $^{-3}$, as can be seen in Figure 4. Models with time-averaged accretion rates between $\langle \dot{M} \rangle = 0.5 - 1.0 \dot{M}_{\text{Edd}}$ have ocean temperatures between $T_b \approx 8.1 \times 10^7 - 1.4 \times 10^8$ K and ocean-crust transition densities between $\rho_t \approx 8.1 \times 10^7 - 2.3 \times 10^8$ g cm $^{-3}$.

3. THE EVOLUTION OF OCEAN g -MODES

The ocean g -modes have been suggested as a possible origin for the observed Z -source NBOs (Bildsten & Cutler 1995) due to their characteristic frequencies between $\approx 5 - 7$ Hz. The thermal g -modes are non-radial oscillations, where the buoyancy arises from entropy gradients in the ocean (McDermott et al. 1983; Bildsten & Cutler 1995). Ocean g -modes may be excited as angular momentum is transported into the ocean by a spreading boundary layer (Inogamov & Sunyaev 1999, 2010), as is the case with acoustic modes in the neutron star

envelope (Philippov et al. 2016). The g -mode spectrum can be analytically approximated (Bildsten & Cutler 1995) by

$$f_{n,l} \approx 2.8 \text{ Hz} \left[\frac{l(l+1)}{6} \frac{T_b}{3 \times 10^7 \text{ K}} \frac{56}{A} \right]^{1/2} \left(\frac{10 \text{ km}}{R} \right) \times \left[1 + \left(\frac{3n\pi}{2} \right)^2 \left(\ln \left\{ \frac{\rho_t}{1 \text{ g cm}^{-3}} \right\} \right)^{-2} \right]^{-1/2}, \quad (4)$$

where n is the number of nodes in the ocean, l is the angular wavenumber, and R is the radius of the neutron star. The upper boundary of the ocean is taken at the base of the envelope near a mass density of $\rho \approx 1 \text{ g cm}^{-3}$, however, the frequency spectrum is largely insensitive to the location of this upper boundary. Even though Equation 4 is derived for an isothermal ocean, the oscillation spectrum is primarily set by the temperature at the base of the ocean in non-isothermal models (Bildsten & Cumming 1998), and Equation 4 gives frequencies accurate within $\approx 10\%$ (Bildsten & Cutler 1995).

Here we examine the predicted fundamental $n = 1$ $l = 2$ g -mode frequency during and after an accretion outburst. Although the $l = 1$ should be more easily observed (Bildsten & Cutler 1995), the mode frequencies are smaller by a factor of $\sqrt{3}$ and are inconsistent with observed NBO frequencies. It is unclear why the fundamental $n = 1$ $l = 2$ mode may be excited preferentially with respect to the $l = 1$ mode. Furthermore, this calculation is only valid for slowly rotating neutron stars with $\nu_{\text{spin}} \ll 300 \text{ Hz}$ and with magnetic fields $B \lesssim 10^{11} \text{ G}$; these limits are consistent with the spin frequencies for the atoll sources inferred from kHz QPOs (e.g., KS 1731-260; Wijnands & van der Klis 1997); though this method for determining ν_{spin} is debated (e.g., Méndez & Belloni 2007). For simplicity, we assume that the Z-sources fall within these limits. Note, however, that at spin frequencies of $\nu_{\text{spin}} \gtrsim f_{n,l}$ the ocean g -modes become highly modified by the rapid rotation of the neutron star and observed NBO frequencies would then only be consistent with g -modes of high radial order (Bildsten et al. 1996).

In a cold ocean ($T_b \approx T_{\text{core}} \sim 10^7 \text{ K}$), the predicted fundamental $n = 1$ $l = 2$ g -mode frequency is $\approx 3 \text{ Hz}$. An increase in the predicted g -mode fundamental frequency is apparent in all Z-sources with $\langle \dot{M} \rangle \gtrsim 0.1 \dot{M}_{\text{Edd}}$ when the ocean reaches steady state. For example, sources with time-averaged accretion rates $\langle \dot{M} \rangle \lesssim 0.5 \dot{M}_{\text{Edd}}$ have predicted fundamental g -mode frequencies between ≈ 3 – 5 Hz and sources with $\langle \dot{M} \rangle \gtrsim 0.5 \dot{M}_{\text{Edd}}$ have predicted frequencies between ≈ 3 – 7 Hz . Note that $\approx 7 \text{ Hz}$ is the maximum $n = 1$, $l = 2$ frequency reached in a model with $\langle \dot{M} \rangle = 1.0 \dot{M}_{\text{Edd}}$, as can be seen in Figure 4.

The predicted g -modes in sources that require shallow heating, however, naturally reach frequencies $\gtrsim 7 \text{ Hz}$, as can be seen in Figure 3. For example, during the MAXI J0556-332 outburst, the predicted fundamental g -mode frequency quickly becomes $\gtrsim 7 \text{ Hz}$ after ≈ 20 days and reaches $\approx 16 \text{ Hz}$ within ≈ 100 days. The predicted fundamental remains at $\approx 16 \text{ Hz}$ for the duration of the outburst and persists at $\approx 16 \text{ Hz}$ for ≈ 500 days into quiescence. The model of the MXB 1659-29 outburst reaches frequencies $\gtrsim 7 \text{ Hz}$ within the first ≈ 30 days of the outburst. The predicted fundamental g -mode frequency approaches $\approx 10 \text{ Hz}$ when the ocean temperature reaches a steady state temperature about ≈ 700 days into the outburst. The model of the XTE J1701-462 outburst behaves similarly to MXB 1659-29, reaching a predicted fundamental g -mode frequency near $\approx 10 \text{ Hz}$ when the ocean

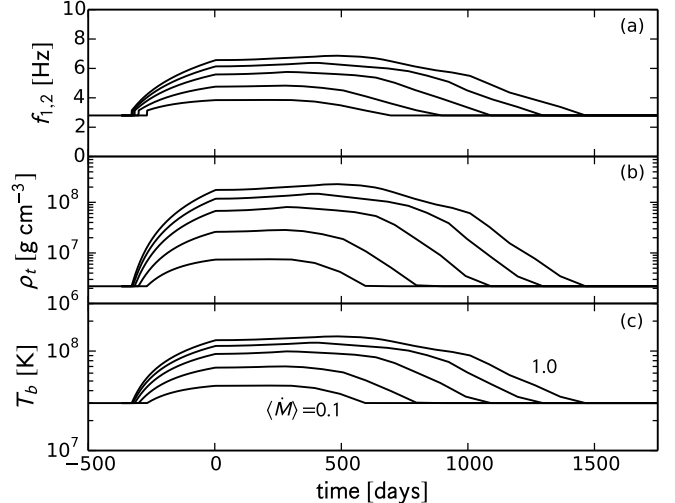


FIG. 4.— Thermal evolution of the ocean as a function of time during outburst/quiescence for accreting models with time-averaged accretion rates $\langle \dot{M} \rangle / \dot{M}_{\text{Edd}} = 0.1, 0.25, 0.5, 0.75, \text{ and } 1.0$. Panel (a): fundamental $n = 1$, $l = 2$ g -mode frequency in the ocean (Equation 4). Panel (b): the ocean-crust transition density (Equation 2). Panel (c): temperature at the ocean-crust transition.

temperature reaches steady-state. The ocean cools relatively slowly in XTE J1701-462, due to its larger impurity parameter of $Q_{\text{imp}} = 7$, taking ≈ 3100 days to cool completely — much longer than MAXI J0556-332 and MXB 1659-29.

4. DISCUSSION

In this study, we investigate the thermal evolution of the transient Z-sources to characterize the temporal evolution of the ocean g -modes during outburst and quiescence. Before accretion begins, the predicted fundamental g -mode is initially $\approx 3 \text{ Hz}$ in the cold ocean ($T_b \approx T_{\text{core}} \sim 10^7 \text{ K}$). During active accretion, the predicted fundamental g -mode frequency increases as unavoidable accretion-driven nuclear heating raises the ocean's temperature. For example, sources accreting between $\langle \dot{M} \rangle = 0.1$ – $1.0 \dot{M}_{\text{Edd}}$ have predicted fundamental g -modes between ≈ 3 – 7 Hz . Predicted fundamental g -mode frequencies $\gtrsim 7 \text{ Hz}$ require active shallow heating during outburst to reach ocean temperatures $\gtrsim 10^8 \text{ K}$ required to support these frequencies. Therefore, observing NBOs $\gtrsim 7 \text{ Hz}$ in transients that require shallow heating, such as MAXI J0556-332, MXB 1659-29, and XTE J1701-462, provides an observational test to link NBOs and the ocean g -modes. In particular, during steady-state accretion, MAXI J0556-332 has predicted fundamental g -mode frequencies between ≈ 8 – 16 Hz , and MXB 1659-29 and XTE J1701-462 have predicted g -mode frequencies between ≈ 8 – 10 Hz — frequencies only possible in the hotter oceans found in sources with shallow heating. We predict that MAXI J0556-332 had a fundamental g -mode frequency near $\approx 11 \text{ Hz}$ at the time of its recent activity (Jin & Kong 2016; Negoro et al. 2016; Russell & Lewis 2016). If shallow heating is active during the current outburst in MXB 1659-29 (Negoro et al. 2015), we predict that this source will have a fundamental g -mode frequency near $\approx 9 \text{ Hz}$ at the time of the most recent observation (Bahramian et al. 2016) after being in outburst for ≈ 160 days.

NBO frequencies observed in the last outburst from XTE J1701-462 (Fridriksson et al. 2010) are consistent with ocean g -modes. NBOs were observed within the first ≈ 10 weeks near $\approx 7 \text{ Hz}$ (Homan et al. 2007), and our model predicts fundamental g -mode frequencies near $\approx 7 \text{ Hz}$ after

10 weeks of active accretion. Furthermore, once the ocean reaches steady state, our model of the XTE J1701-462 outburst contains predicted ocean g -modes between ≈ 7 –10 Hz, which is consistent with the observed ≈ 7 –9 Hz NBOs observed in this source during outburst (Homan et al. 2010).

Although current instrumentation may not allow observations of NBOs in MXB 1659-29 and MAXI J0556-332 during quiescence, renewed accretion outbursts in both objects may allow observations of NBOs. We predict that observed NBOs during these sources current accretion outbursts should be ≥ 5 Hz in MXB 1659-29 and ≥ 10 Hz in MAXI J0556-332. The renewed activity in MAXI J0556-332 (Negoro et al. 2016; Russell & Lewis 2016) perhaps holds the best prospects for catching large NBO frequencies because the ocean in MAXI J0556-332 had not cooled to the core temperature before the most recent accretion outburst, and the predicted ocean g -mode frequency is already ≥ 7 Hz.

Note that the above observational tests for the presence of ocean g -modes does not require a complete picture of how X-ray emission is modulated by ocean oscillations, which is outside the scope of this work. Uncertainties remain in the nature of the accretion flow near the neutron star surface and how the accretion flow may interact with the neutron star's outer layers. For example, a spreading boundary layer of accreted material may extend into the ocean (Inogamov & Sunyaev 1999, 2010), and may transport angular momentum therein. A coupling of the boundary layer and the ocean in this way may only modulate X-ray emission near the equator, however, where modes may even interfere with accretion disk emission (Bildsten et al. 1996). If observations support a g -mode origin for the NBOs, this will motivate future work to model the ocean's coupling to a spreading boundary layer.

If NBOs are indeed ocean g -modes, observed NBO frequencies ≥ 7 Hz can then be used as a diagnostic of the shallow heating strength. For example, as shown in this work, ocean g -mode frequencies near ≈ 10 Hz (≈ 16 Hz) are found in sources in steady state with $Q_{\text{shallow}} \approx 1$ MeV ($Q_{\text{shallow}} \approx 6$ MeV). It is worth noting, however, that during outburst the ocean in MAXI J0556-332 approaches a maximum temperature set by neutrino emission around $T_b \approx 2 \times 10^9$ K at the depth of the shallow heat source (Deibel et al. 2015). Because the ocean temperature is near maximum, a g -mode frequency of ≈ 16 Hz is likely the largest $n = 1$ $l = 2$ g -mode that can be supported in Z-source oceans. Therefore, NBO frequencies of ≈ 16 Hz only give the lower limit $Q_{\text{shallow}} \geq 6$ MeV for the shallow heating strength.

The depth of the ocean-crust transition during outburst is relevant to the study of the shallow heating mechanism. For example, the ocean-crust interface in MAXI J0556-332 moves to densities between $\rho_t \sim 10^9$ – 10^{11} g cm $^{-3}$ during outburst. This density range is characteristic of the location of the shallow heating inferred from quiescent light curves of quasi-persistent transients (Brown & Cumming 2009), which is needed at mass densities near $\rho_{\text{shallow}} \lesssim 3 \times 10^{10}$ g cm $^{-3}$. For example, shallow heating is required between $\rho_{\text{shallow}} \sim$

5×10^9 – 3×10^{10} g cm $^{-3}$ in MAXI J0556-332, as determined from its quiescent light curve (Deibel et al. 2015). This suggests that the shallow heating mechanism is connected to the ocean-crust phase transition, and work in this direction is ongoing.

Often the observed ≈ 5 –7 Hz NBOs blend into ≈ 10 –20 Hz flaring branch oscillations (hereafter FBOs); for example, a continuous blending was observed in SCO X-1 (Casella et al. 2006). The timescale of observed NBO-FBO blending disfavors a g -mode origin for the FBOs. The thermal time at the depth of the ocean-crust transition (Figure 2) determines the timescale for variations in the g -mode frequencies. For g -mode frequencies $\lesssim 7$ Hz, variations may occur on timescales of hours; variations in frequencies ≥ 7 Hz occur on timescales of days — much longer than the timescale of the observed blending. The NBO-FBO blending phenomena, however, is consistent with a superposition of ocean g -modes and ocean interface waves. The interface modes were determined to have frequencies of ~ 200 Hz when calculated with a rigid crust boundary condition (McDermott et al. 1988), but may have lower frequencies near ~ 20 Hz when the flexibility of the crust is taken into account (Piro & Bildsten 2005). It is unclear why oscillation energy might transition between the different modes, but the coupling of the g -modes to the interface modes is worthy of future study.

Quasi-periodic oscillations between ≈ 5 –7 Hz in the atoll sources ($L_X \sim 0.1$ – $0.5 L_{X,\text{Edd}}$) are also consistent with ocean g -modes. For example, the ≈ 7 Hz oscillation observed in 4U 1820-30 (Wijnands et al. 1999; Belloni et al. 2004) is consistent with a $n = 1$ $l = 2$ g -mode in a lighter ocean. In a lighter ocean, such as those considered in Bildsten & Cutler (1995), g -mode frequencies are larger by a factor of $\sim (56/16)^{1/2}$ compared to those studied in this work. This may explain the observed oscillations in 4U 1820-30, where accretion from the helium companion star (Wijnands et al. 1999) would result in a different ocean composition than the one considered here.

A.D. thanks Andrew Cumming and Edward Brown for insightful comments on the manuscript. A.D. thanks Jeroen Homan for useful discussions on the nature of Z-sources and Bob Rutledge for the encouragement to publish work on the neutron star ocean. Support for A.D. was provided by the National Aeronautics and Space Administration through *Chandra* Award Number TM5-16003X issued by the *Chandra X-ray Observatory* Center, which is operated by the Smithsonian Astrophysical Observatory for and on behalf of the National Aeronautics and Space Administration under contract NAS8-03060. A.D. is also supported by the National Science Foundation under grant No. AST-1516969 and the Michigan State University College of Natural Science Dissertation Completion Fellowship. This material is based upon work supported by the National Science Foundation under grant No. PHY-1430152 (Joint Institute for Nuclear Astrophysics - Center for the Evolution of the Elements).

REFERENCES

- Bahramian, A., Heinke, C. O., Wijnands, R., & Degenaar, N. 2016, *The Astronomer's Telegram*, 8699, 1
- Bardeen, J. M., & Petterson, J. A. 1975, *ApJ*, 195, L65
- Belloni, T., Parolin, I., & Casella, P. 2004, *A&A*, 423, 969
- Bildsten, L., & Cumming, A. 1998, *ApJ*, 506, 842
- Bildsten, L., & Cutler, C. 1995, *ApJ*, 449, 800
- Bildsten, L., Ushomirsky, G., & Cutler, C. 1996, *ApJ*, 460, 827
- Bisnovatyi-Kogan, G. S., & Chechetkin, V. M. 1979, *Soviet Physics Uspekhi*, 22, 89
- Brown, E. F. 2015, *dStar: Neutron star thermal evolution code*, *Astrophysics Source Code Library*, ascl:1505.034
- Brown, E. F., Bildsten, L., & Rutledge, R. E. 1998, *ApJ*, 504, L95
- Brown, E. F., & Cumming, A. 2009, *ApJ*, 698, 1020

- Cackett, E. M., Brown, E. F., Cumming, A., Degenaar, N., Miller, J. M., & Wijnands, R. 2010, *ApJ*, 722, L137
- Cackett, E. M., Wijnands, R., Miller, J. M., Brown, E. F., & Degenaar, N. 2008, *ApJ*, 687, L87
- Casella, P., Belloni, T., & Stella, L. 2006, *A&A*, 446, 579
- Degenaar, N., Wijnands, R., Wolff, M. T., et al. 2009, *MNRAS*, 396, L26
- Degenaar, N., Medin, Z., Cumming, A., et al. 2014, *ApJ*, 791, 47
- Degenaar, N., Wijnands, R., Bahramian, A., et al. 2015, *MNRAS*, 451, 2071
- Deibel, A., Cumming, A., Brown, E. F., & Page, D. 2015, *ApJ*, 809, L31
- Dubus, G., Kern, B., Esin, A. A., Rutledge, R. E., & Martin, C. 2004, *MNRAS*, 347, 1217
- Farouki, R. T., & Hamaguchi, S. 1993, *Phys. Rev. E*, 47, 4330
- Fridriksson, J. K., Homan, J., & Remillard, R. A. 2015, *ApJ*, 809, 52
- Fridriksson, J. K., Homan, J., Wijnands, R., et al. 2010, *ApJ*, 714, 270
- Fridriksson, J. K., Homan, J., Wijnands, R., et al. 2011, *ApJ*, 736, 162
- Gupta, S., Brown, E. F., Schatz, H., Möller, P., & Kratz, K.-L. 2007, *ApJ*, 662, 1188
- Haensel, P., & Zdunik, J. L. 1990, *A&A*, 227, 431
- Haensel, P., & Zdunik, J. L. 2003, *A&A*, 404, L33
- Haensel, P., & Zdunik, J. L. 2008, *A&A*, 480, 459
- Hasinger, G., & van der Klis, M. 1989, *A&A*, 225, 79
- Hertz, P., Vaughan, B., Wood, K. S., et al. 1992, *ApJ*, 396, 201
- Homan, J. 2012, *ApJ*, 760, L30
- Homan, J., Fridriksson, J. K., & Remillard, R. A. 2015, *ApJ*, 812, 80
- Homan, J., Fridriksson, J. K., Wijnands, R., Cackett, E. M., Degenaar, N., Linares, M., Lin, D., & Remillard, R. A. 2014, *ApJ*, 795, 131
- Homan, J., Linares, M., van den Berg, M., & Fridriksson, J. 2011, *The Astronomer's Telegram*, 3650, 1
- Homan, J., van der Klis, M., Fridriksson, J. K., et al. 2010, *ApJ*, 719, 201
- Homan, J., van der Klis, M., Wijnands, R., et al. 2007, *ApJ*, 656, 420
- Inogamov, N. A., & Sunyaev, R. A. 1999, *Astronomy Letters*, 25, 269
- Inogamov, N. A., & Sunyaev, R. A. 2010, *Astronomy Letters*, 36, 848
- Jin, R., & Kong, A. K. H. 2016, *The Astronomer's Telegram*, 8530, 1
- Jonker, P. G., van der Klis, M., Homan, J., et al., 2002, *MNRAS*, 333, 665
- Kuulkers, E., van der Klis, M., Oosterbroek, T., et al., 1994, *A&A*, 289, 795
- Lense, J., & Thirring, H. 1918, *Physikalische Zeitschrift*, 19, 156
- Lin, D., Remillard, R. A., & Homan, J. 2009, *ApJ*, 696, 1257
- Matsumura, T., Negoro, H., Suwa, F., et al. 2011, *The Astronomer's Telegram*, 3102, 1
- McDermott, P. N., van Horn, H. M., & Hansen, C. J. 1988, *ApJ*, 325, 725
- McDermott, P. N., van Horn, H. M., & Scholl, J. F. 1983, *ApJ*, 268, 837
- Méndez, M., & Belloni, T. 2007, *MNRAS*, 381, 790
- Negoro, H., Furuya, K., Ueno, S., et al., 2015, *The Astronomer's Telegram*, 7943, 1
- Negoro, H., Nakajima, M., Fujiwara, T., et al., 2016, *The Astronomer's Telegram*, 8513, 1
- Page, D., & Reddy, S. 2013, *Physical Review Letters*, 111, 241102
- Paxton, B., Bildsten, L., Dotter, A., Herwig, F., Lesaffre, P., & Timmes, F. 2011, *ApJS*, 192, 3
- Paxton, B., Cantiello, M., Arras, P., et al. 2013, *ApJS*, 208, 4
- Paxton, B., Marchant, P., Schwab, J., et al. 2015, *ApJS*, 220, 15
- Philippov, A. A., Rafikov, R. R., & Stone, J. M. 2016, *ApJ*, 817, 62
- Piro, A. L., & Bildsten, L. 2005, *ApJ*, 619, 1054
- Potekhin, A. Y., & Chabrier, G. 2000, *Phys. Rev. E*, 62, 8554
- Russell, D. M., & Lewis, F. 2016, *The Astronomer's Telegram*, 8517
- Sato, K. 1979, *Progress of Theoretical Physics*, 62, 957
- Steiner, A. W. 2012, *Phys. Rev. C*, 85, 055804
- Stella, L., & Vietri, M. 1998, *ApJ*, 492, L59
- Strohmayer, T. E. 1993, *ApJ*, 417, 273
- Sugizaki, M., Yamaoka, K., Matsuoka, M., et al. 2013, *PASJ*, 65, 58
- Titarchuk, L., Seifina, E., & Shrader, C. 2014, *ApJ*, 789, 98
- Turlione, A., Aguilera, D. N., & Pons, J. A. 2015, *A&A*, 577, A5
- van der Klis, M., Swank, J. H., Zhang, W., et al., 1996, *ApJ*, 469, L1
- Wijnands, R., Guainazzi, M., van der Klis, M., & Meéndez, M. 2002, *ApJ*, 573, L45
- Wijnands, R., Homan, J., Miller, J. M., & Lewin, W. H. G. 2004, *ApJ*, 606, L61
- Wijnands, R., Miller, J. M., Markwardt, C., Lewin, W. H. G., & van der Klis, M. 2001, *ApJ*, 560, L159
- Wijnands, R., Nowak, M., Miller, J. M., Homan, J., Wachter, S., & Lewin, W. H. G. 2003, *ApJ*, 594, 952
- Wijnands, R., van der Klis, M., & Rijkhorst, E.-J. 1999, *ApJ*, 512, L39
- Wijnands, R. A. D., & van der Klis, M. 1997, *ApJ*, 482, L65
- Wijnands, R. A. D., van der Klis, M., Kuulkers, E., Asai, K., & Hasinger, G. 1997, *A&A*, 323, 399